Available online at www.sciencedirect.com
ScienceDirect
C. R. Mecanique 335 (2007) 113–118
COMPTES RENDUS MECANIQUE
http://france.elsevier.com/direct/CRAS2B/

# Natural convection flow in a tall enclosure using a multigrid method

Nader Ben Cheikh *, Brahim Ben Beya, Taieb Lili

*Faculté des Sciences de Tunis, Département de Physique, Campus Universitaire 2092 El-Manar II, Tunisia*

Received 30 April 2006; accepted after revision 23 January 2007

Available online 26 February 2007

Presented by Sébastien Candel

**Abstract**

A two-dimensional numerical study of natural convection flow in an air filled enclosure of aspect ratio $A = 9$ is investigated in this Note. The numerical method is based on a second order finite volume scheme and a projection method. A full multigrid technique is used to accelerate the convergence of the Poisson pressure equation. The multigrid procedure is briefly described and the critical Rayleigh number above which the flow becomes unsteady is determined. ***To cite this article: N. Ben Cheikh et al., C. R. Mecanique 335 (2007).***



**Résumé**

**Écoulement de convection naturelle dans une longue cavité à l'aide d'une méthode multigrille.** Nous présentons dans ce papier une étude numérique de convection naturelle bidimensionnelle dans une cavité de rapport de forme $A = 9$, remplie d'air. La méthode numérique est basée sur un schéma de type volumes finis du second ordre et une méthode de projection. Une approche multigrille est utilisée pour accélérer la convergence de l'équation de Poisson. La méthode est brièvement décrite et le nombre de Rayleigh critique au-delà duquel l'écoulement devient instationnaire est déterminé. ***Pour citer cet article : N. Ben Cheikh et al., C. R. Mecanique 335 (2007).***



*Keywords:* Computational fluid mechanics; Natural convection flow; Multigrid technique

*Mots-clés :* Mécanique des fluides numérique ; Écoulement de convection naturelle ; Approche multigrille

## 1. Introduction

Accurate solutions of the incompressible Navier–Stokes/Boussinesq equations (NSBE) are of considerable interest in many industrial flows, such as speed aerodynamics and hydrodynamics. The application of computational fluid dynamics methods in these areas shows that for sufficient accuracy, large grid sizes are needed for capturing thin boundary layer properties, detecting high heat transfer spots or resolving small eddy regions. Because of that need, procedures for solving the NSBE, in acceptable CPU times, are at the heart of large scale computations.

* Corresponding author.
*E-mail address:* nader_bc@yahoo.fr (N. Ben Cheikh).

1631-0721/$ – see front matter 
doi:10.1016/j.crme.2007.01.004

So far, one of the most popular techniques for solving the unsteady NSBE may be the use of multigrid methods (MG) [1]. The applications of MG methods have indeed shown nearly optimum convergence characteristics [2–4]. The computation times are directly proportional to the number of grid points, allowing very fine grids to be used and therefore more accurate solutions to be obtained.

In this Note a finite volume, full multi-grid method (FMG) applied to natural convection flows is utilised. The smoother used is the iterative red and black successive over relaxation scheme (RBSOR) [5]. In order to accelerate the convergence, an acceleration parameter is implemented in the classical FMG procedure. It was indeed demonstrated in Ref. [6] that convergence could be substantially improved by just multiplying the correction field in the FMG procedure by some suitable factor $\Gamma > 0$ (AFMG method).

In the next section the numerical approach and the AFMG method are briefly described. Next, the implementation of the AFMG algorithm is validated by a time dependent benchmark problem of natural convection in a tall cavity of aspect ratio 8 [7,8]. The method is then applied to study natural convection in an enclosure of aspect ratio 9 and to determine the critical Rayleigh above which the flow becomes unsteady. In the final section the most important findings of this study are summarized.

## 2. Numerical approach

The non-dimensional governing equations for an incompressible flow, corresponding to the continuity, Navier–Stokes and energy equations, under the Boussinesq approximation, are given by:

$$\frac{\partial u_i}{\partial x_i} = 0 \tag{1}$$

$$\frac{\partial u_i}{\partial t} + \frac{\partial (u_j u_i)}{\partial x_j} = -\frac{\partial p}{\partial x_i} + \sqrt{\frac{Pr}{Ra}} \frac{\partial^2 u_i}{\partial x_j \partial x_j} + \theta \delta_{i2} \tag{2}$$

and

$$\frac{\partial \theta}{\partial t} + \frac{\partial (u_i \theta)}{\partial x_i} = \frac{1}{\sqrt{Ra\,Pr}} \frac{\partial^2 \theta}{\partial x_i \partial x_i} \quad (i = 1, 2) \tag{3}$$

where $u_i = (u, v)$, $p$ and $\theta$ are the velocity, the kinematic pressure, and temperature, respectively. Here $\delta_{ij}$ is the Krönecker symbol. Eqs. (1)–(3) where obtained using the characteristic length $W$, velocity scale $u_0 = \sqrt{g\beta W \Delta T}$, time scale $t_0 = W/u_0$ and pressure scale $p_0 = \rho u_0^2$. $\rho$ is the mass density, $g$ the gravitational acceleration, and $\beta$ the isobaric coefficient of thermal expansion. The non-dimensional temperature $\theta$ is defined in terms of the wall temperature difference and a reference temperature:

$$\theta = \frac{T - T_r}{T_h - T_c}$$

$T_h$ is the temperature of the hot wall, and $T_c$ is that of the cold wall. The non-dimensional parameters are the Rayleigh number ($Ra$) and the Prandtl number ($Pr$) defined as $Ra = g\beta \Delta T W^3/(\nu\alpha)$ and $Pr = \nu/\alpha$ , where $\nu$ is the kinematic viscosity, $\alpha$ the thermal diffusivity, and $\Delta T = T_h - T_c$ the temperature difference between the hot and cold walls.

The unsteady Navier–Stokes and energy equations are discretized by a second-order time stepping of finite difference type. Non-linear terms in Eq. (2) are treated explicitly with a second-order Adams–Bashforth scheme. Convective terms in Eq. (3) are treated semi-implicitly and diffusion terms in both Eqs. (2) and (3) are treated implicitly.

In order to get round the difficulty that resides in the strong velocity-pressure coupling, we choose to use a projection method [9,10]. Using this method, the global algorithm consists of:

- solving at a first step Eq. (4) related to the energy equation:

$$\frac{3\theta^{n+1} - 4\theta^n + \theta^{n-1}}{2\Delta t} + \frac{\partial [(2u_i^n - u_i^{n-1})\theta^{n+1}]}{\partial x_i} = \frac{1}{\sqrt{Ra\,Pr}} \frac{\partial^2 \theta^{n+1}}{\partial x_i \partial x_i} \tag{4}$$

- the temperature field $\theta^{n+1}$ permits the solution of the system of Eqs. (5) related to an intermediate velocity field $u_i^*$ that may not be divergence free:

$$\frac{3u_i^* - 4u_i^n + u_i^{n-1}}{2\Delta t} + 2\frac{\partial(u_j u_i)^n}{\partial x_j} - \frac{\partial(u_j u_i)^{n-1}}{\partial x_j} = -\left(\frac{\partial p}{\partial x_i}\right)^n + \sqrt{\frac{Pr}{Ra}}\frac{\partial^2 u_i^*}{\partial x_j \partial x_j} + \theta^{n+1}\delta_{i2} \tag{5}$$

- the obtained intermediate velocity field permits to solve the Poisson equation:

$$\frac{\partial^2 \phi}{\partial x_i \partial x_i} = \frac{\partial u_i}{\partial x_i} \tag{6}$$

  where $\phi$ is an arbitrary scalar field;
- once $u_i^*$ and $\phi$ are obtained, the real velocity field and the pressure are updated by the following expressions:

$$u_i^{n+1} = u_i^* - \frac{\partial \phi}{\partial x_i} \tag{7}$$

$$p^{n+1} = p^n + \frac{3\phi}{2\Delta t} - \sqrt{\frac{Pr}{Ra}}\left(\frac{\partial^2 \phi}{\partial x_i \partial x_i}\right) \tag{8}$$

A second order finite-volume method [11] is used to discretize the Navier–Stokes and energy equations. Thus, equations to solve are the equation of energy, the equation related to an intermediate velocity field and a Poisson equation. The two first equations are solved using the red and black successive over-relaxation method (RBSOR) [5], while the Poisson pressure correction equation is solved using an accelerated full multigrid method (AFMG) with the RBSOR method as a smoother. The main idea of the multigrid method can be found in Refs. [1,2]. We have implemented our multigrid procedure in a so-called full multigrid (FMG) fashion [2]. Indeed, before starting V-cycles, the source term is calculated on the coarsest grid permitting the determination of an exact solution. This solution is progressively interpolated from the coarsest to the finest grid, used there as a starting guess for the V-cycle procedure. In order to optimize the number of V-cycles, it is demonstrated [6] that convergence can be substantially improved by just multiplying the correction field in the multigrid procedure by some suitable factor $\Gamma > 0$ (AFMG method). Several tests showed that for $\Gamma = 3.75$ and after a short time of integration, only one to two V-cycles are necessary to satisfy the convergence.

## 3. Results and discussion

### 3.1. Code validation

As a test case we considered the time dependent solution for an 8:1 differentially heated cavity. The benchmark description and the physical problem are well detailed in Ref. [7]. Thus, in this paragraph, results related to $Ra = 3.4 \times 10^5$, $Pr = 0.71$ and $A = H/W = 8$ are presented. Here, $H$ and $W$ are the height and the width of the enclosure, respectively. The number of control volumes applied on the finest grid is $96 \times 480$ corresponding to 6 levels in the multigrid calculation. The coarsest grid level consisted thus of $3 \times 15$ number of control volumes. Cartesian grids are uniform in the vertical direction and non-uniform in the horizontal direction with smallest cells near hot and cold walls, respectively.

We ran the computations on three different grids with increasing refinement: $24 \times 120$ nodes (coarse), $48 \times 240$ nodes (medium) and $96 \times 480$ nodes (fine). Tests on a coarse and a medium grid, respectively, $24 \times 120$ and $48 \times 240$ (corresponding to 4 and 5 levels in the multigrid calculations), were first carried on to determine an optimal value of factor $\Gamma$. On both grids, a mean value of $\Gamma = 3.75$ was obtained assuming that the value of $\Gamma$ is grid independent.

According to the CFL criterion, time steps on grids $24 \times 120$, $48 \times 240$ and $96 \times 480$ were fixed at $\Delta t = 3.2 \times 10^{-2}$, $\Delta t = 1.6 \times 10^{-2}$ and $\Delta t = 8 \times 10^{-3}$, respectively. Computational results were obtained for each of the three grid types and simulations were run until a non-dimensional time of $t = 1500$.

During the flow solution, time history data at point 1, i.e., ($x = 0.181$; $y = 7.37$), in the cavity were reported at each time step. Table 1 provides a summary of the time-history data for the three grid resolutions. The table presents information (at point 1) for the velocity in the $x$-direction ($u_1$), the velocity in the $y$-direction ($v_1$), the temperature ($\theta_1$) and the Nusselt number ($Nu$). The corresponding fluctuating $x$-velocity, $y$-velocity, temperature, and Nusselt number are $\Delta u_1$, $\Delta v_1$, $\Delta\theta_1$, and $\Delta Nu$. The period, $\tau_\theta$, is the period associated with the temperature oscillation at point 1.

Table 1
Comparison of the time-averaged data and the corresponding fluctuations at point 1

Tableau 1
Comparaison des grandeurs moyennes et fluctuations correspondantes au point 1

| Quantity | Grid resolution | | |
|---|---|---|---|
| | $24 \times 120$ | $48 \times 240$ | $96 \times 480$ |
| $u_1$ | $5.01203 \times 10^{-2}$ | $5.37072 \times 10^{-2}$ | $5.61780 \times 10^{-2}$ |
| $\Delta u_1$ | $7.16083 \times 10^{-4}$ | $3.59755 \times 10^{-2}$ | $5.43379 \times 10^{-2}$ |
| $v_1$ | $4.52762 \times 10^{-1}$ | $4.59891 \times 10^{-1}$ | $4.61412 \times 10^{-1}$ |
| $\Delta v_1$ | $1.12033 \times 10^{-3}$ | $5.28620 \times 10^{-2}$ | $7.67392 \times 10^{-2}$ |
| $\theta_1$ | $2.68107 \times 10^{-1}$ | $2.66011 \times 10^{-1}$ | $2.65582 \times 10^{-1}$ |
| $\Delta\theta_1$ | $5.93518 \times 10^{-4}$ | $2.88141 \times 10^{-2}$ | $4.26336 \times 10^{-2}$ |
| $Nu$ | 4.61383 | 4.58802 | 4.58179 |
| $\Delta Nu$ | $1.70366 \times 10^{-4}$ | $4.98058 \times 10^{-3}$ | $7.10453 \times 10^{-3}$ |
| $\tau_\theta$ | 3.7440 | 3.4400 | 3.4160 |

In order to compare the performances of contributions to the benchmark problem, a number of metrics based on some of the quantities shown in Table 1 were defined in Ref. [7]. The values obtained by each participant were compared against the accepted values of Xin and Le Quéré [8], and the deviations from these latter values defined the metrics. Hence, values as close to zero as possible are the 'target'. Here, we present our performance, based on the overall metric, $E$, defined by:

$$E = \frac{\bar{\varepsilon}_{\theta_1} + \bar{\varepsilon}_{u_1} + \bar{\varepsilon}_{Nu_1} + \varepsilon_{\tau_\theta} + \varepsilon'_{\theta_1} + \varepsilon'_{u_1} + \varepsilon'_{Nu_1}}{7} \tag{9}$$

which represents the average of the errors computed in the period, mean velocity, temperature and Nusselt number, and the corresponding error in the oscillation amplitudes. This metric has been calculated on the grid $96 \times 480$ for $1465.84 \leqslant t \leqslant 1500$ (ten periods) and compared with some of the contributors to the MIT session (see Table 2). As seen, our metric is ranked first, meaning that the numerical method is very efficient giving results very close to the 'true' solution provided by Xin and Le Quéré [8].

In order to reflect the computational cost required to obtain the solution, a normalized algorithm timing defined as:

$$\eta_{AT} = \left(\frac{m \sec}{node.step} . \frac{steps}{period}\right) . specFP95 \tag{10}$$

was proposed in Ref. [7]. This normalized performance metric is scaled in a relative sense so that the minimum value of $\eta_{AT}$ is unity. Our metric measured on a Dell Dimension 4600 system, with a single 2.9 GHz processor ($specFP95 = 71$), is presented in Table 3 and is compared with some of the contributors to the MIT session. As it can be seen, the value is ranked fourth, meaning that the method is quite fast.

Table 2
Comparison of overall metric $E$

Tableau 2
Comparaison du métrique $E$

| First author [7] | $E$ | Rank order |
|---|---|---|
| Present study | 0.2491 | 1 / (31) |
| Johnston | 0.3352 | 2 / (31) |
| Davis | 0.5631 | 3 / (31) |
| Armfield | 0.9375 | 7 / (31) |
| Christon | 0.9849 | 9 / (31) |
| Westerberg | 2.7708 | 15 / (31) |
| Bruneau | 9.5773 | 21 / (31) |
| Chan | 21.266 | 27 / (31) |

Table 3
Comparison of the normalized algorithm timing metric

Tableau 3
Comparaison du métrique du temps algorithmique normalisé

| First author [7] | $\eta_{AT}$ | Ranking |
|---|---|---|
| Johnston | 1.00 | 1 / (26) |
| Christon II | 1.31 | 2 / (26) |
| Christon III | 1.35 | 3 / (26) |
| Pres. Study | 2.11 | 4 / (26) |
| Matsumoto | 2.34 | 5 / (26) |
| Bruneau | 3.40 | 6 / (26) |
| Armfield | 85.14 | 22 / (26) |
| Le Quéré | 90.17 | 24 / (26) |
| Ingberg | 2010.14 | 26 / (26) |

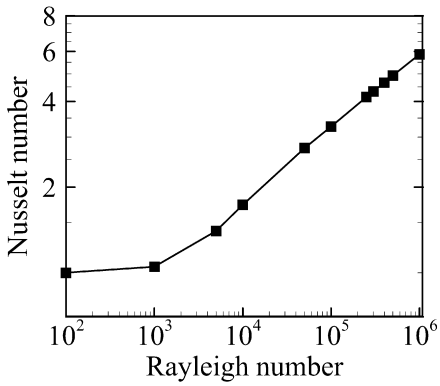


Fig. 1. Nusselt number versus Rayleigh.

Fig. 1. Nombre de Nusselt en fonction du Rayleigh.

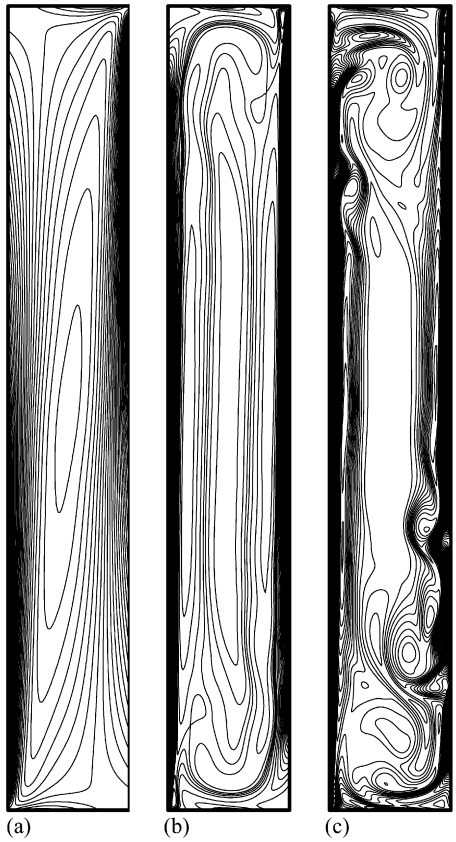


Fig. 2. Vorticity isolines for: (a) $Ra = 10^4$, (b) $Ra = 3.4 \times 10^5$ and (c) $Ra = 10^6$.

Fig. 2. Iso-vorticités pour : (a) $Ra = 10^4$, (b) $Ra = 3.4 \times 10^5$ and (c) $Ra = 10^6$.

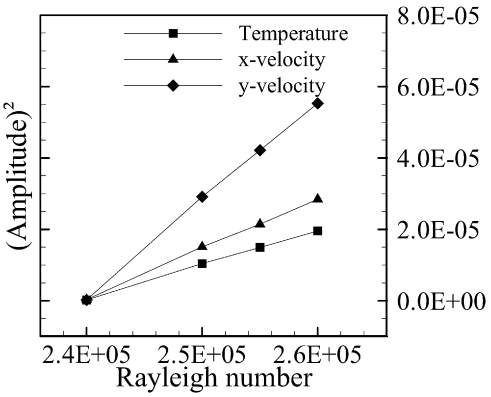


Fig. 3. (Amplitude)$^2$ versus Rayleigh.

Fig. 3. (Amplitude)$^2$ en fonction du Rayleigh.

### *3.2. Natural convection in a 9:1 heated enclosure*

We here consider the problem of a differentially heated closed cavity of aspect ratio $A = 9$. The numerical results are obtained for Rayleigh numbers ranging from $Ra = 10^2$ to $Ra = 10^6$ and a Prandtl number of $Pr = 0.71$.

A proportional number of control volumes according to the 8:1 heated enclosure case described above was applied, i.e., $96 \times 520$ nodes. During the flow solution, time history data at point 2 of coordinate ($x = 0.15$; $y = 7.75$) were reported at each time step.

The results showed that for Rayleigh numbers lower than $Ra = 10^5$, the flow was still steady and for Rayleigh numbers somewhat greater than $2 \times 10^5$ the flow bifurcates to an unsteady periodic state, followed by a chaotic state if Rayleigh number was till increased.

In Fig. 1 the average Nusselt number, $Nu$, is plotted versus the Rayleigh number. As expected, the Nusselt number increases with $Ra$ and for Raleigh numbers lower than $10^3$, $Nu$ is very weak and therefore diffusion is the principal mode of heat transfer. For $Ra$ greater than $5 \times 10^4$, the intensity of convection increases and in the range $5 \times 10^4 \leqslant Ra \leqslant 10^6$, $Nu$ can be expressed through the following correlation:

$$Nu = 0.178 Ra^{0.252} \tag{11}$$

Fig. 2 shows the instantaneous iso-vorticity features of the flow for three Rayleigh numbers related to a steady, a periodic and a chaotic state, obtained for $Ra = 10^4$, $Ra = 3.4 \times 10^5$ and $Ra = 10^6$, respectively. As seen, by increasing the Rayleigh number, a more complex solution is found and an increase of vortex dynamics is observed. Note that the period of the flow at $Ra = 3.4 \times 10^5$ has been calculated, and comparing to the 8:1 benchmark problem, a smaller value of $\tau_\theta = 3.120$ was found.

The determination of the critical Rayleigh number, $Ra_c$, was determined using the same method as presented in Ref. [12]. In fact, the solution of a supercritical Hopf bifurcation is proportional to $\sqrt{Ra - Ra_c}$. Hence, in Fig. 3, we report amplitudes squared, $(Amp)^2$, of quantities $\theta_2$, $u_2$ and $v_2$ at point 2 versus the Rayleigh number. By extrapolating results at $Amp = 0$, we obtained an approximate value of $Ra_c = 2.4 \times 10^5$. Comparing that value with proposed ones related to the benchmark enclosure of aspect ratio $A = 8$ ($Ra_c \sim 3.0 \times 10^5$), a decrease of the critical Rayleigh number may be observed by increasing the aspect ratio.

## 4. Conclusion

In this Note, a numerical method for solving the Navier–Stokes/Boussinesq equations has been investigated. The numerical method is based on a finite volume approach, a projection method and an accelerated full-multigrid technique (AFMG). The performed test calculations demonstrated the potential of the method for enabling very accurate solutions on very fine grids in acceptable CPU times. Tests showed that a mean value for acceleration parameter $\Gamma$ of 3.75 was well appropriated for natural convection flows in differentially heated enclosures. Using the AFMG method, a study in an enclosure of aspect ratio $A = 9$ was investigated. For Rayleigh numbers ranging from $10^4$ to $10^6$, a correlation between Nusselt number and Rayleigh number has been reported. The supercritical solution was also determined giving an approximate critical Rayleigh number of $Ra_c = 2.4 \times 10^5$.

## References

[1] W. Hackbusch, Multigrid Methods and Applications, Springer-Verlag, Berlin/New York, 1985.
[2] M. Hortmann, M. Peric, G. Scheuerer, Finite volume multigrid prediction of laminar natural convection: bench-mark solutions, Int. J. Numer. Methods Fluids 11 (1990) 189–207.
[3] E. Nobile, Simulation of time-dependent flow in cavities with the additive-correction multigrid method, Part I: Mathematical formulation, Numer. Heat Transfer B 30 (1996) 341–350.
[4] A. Brandt, Multi-level adaptive solutions to boundary-value problems, Math. Comput. 31 (1977) 333–390.
[5] R. Barrett, et al., Templates for the Solution of Linear Systems: Building Blocks for Iterative Methods, SIAM, 1994.
[6] D. Braess, Towards algebraic multigrid for elliptic problems of second order, Computing 55 (1995) 379–393.
[7] M.A. Christon, P.M. Gresho, S.B. Sutton, Computational predictability of time-dependent natural convection flows in enclosures (including a benchmark solution), Int. J. Numer. Methods Fluids 40 (2002) 953–980.
[8] S. Xin, P. Le Quéré, An extended Chebyshev pseudo-spectral benchmark for the 8:1 differentially heated cavity, Int. J. Numer. Methods Fluids 40 (2002) 981–998.
[9] R. Peyret, T.D. Taylor, Methods for Fluid Flow, Springer-Verlag, Berlin/New York, 1983.
[10] Y. Achdou, J.L. Guermond, Convergence analysis of a finite element projection/Lagrange–Galerkin method for the incompressible Navier–Stokes equations, SIAM J. Numer. Anal. 37 (2000) 799–826.
[11] S.V. Patankar, Numerical Heat Transfer and Fluid Flow, McGraw-Hill, New York, 1980.
[12] H. Wang, S. Xin, P. Le Quéré, Étude numérique du couplage de la convection naturelle avec le rayonnement de surfaces en cavité carrée remplie d'air, C. R. Mécanique 334 (2006) 48–57.